Surface Modification of Erbium-Doped Silicon Nanocrystals

Junmin Ji, Yandong Chen, Robert A. Senter, and Jeffery L. Coffer*

Department of Chemistry, Texas Christian University, Ft. Worth, Texas 76129

Received June 26, 2001. Revised Manuscript Received September 20, 2001

This work describes a viable route to the surface chemical modification of erbium-doped silicon nanocrystals via their reaction with a capping reagent immediately after their formation in a pyrolysis oven. While the derivatized, doped nanocrystals retain the desired luminescence at 1540 nm associated with the erbium centers, for the $-SiMe_3$- and $-Si(CH_2)_3CN$-capped nanocrystals, there is a clear improvement in their solubility in solvents such as butylphenyl ether. In contrast, propylamine-modified surfaces become less soluble in the solvents tested, presumably as a consequence of extensive hydrogen-bonding-induced aggregation. The implications of these modified nanocrystals for other applications are also discussed.

Introduction

Silicon remains the elemental semiconductor of choice in modern electronic devices. Yet its fundamental electronic structure, specifically an indirect band gap, limits its applicability in optoelectronic platforms envisioned for future structures of even smaller dimensions.[1] Rare earth incorporation into crystalline Si is an appealing strategy in this regard because of the relatively narrow line widths of its luminescence and an insensitivity to host matrix.[2−5] Erbium is of particular interest for this approach because its $(^4I_{13/2}) \rightarrow (^4I_{15/2})$ luminescent transition at 1.54 μm lies at a transmission maximum for silica-based waveguides.

Methods devised to achieve erbium incorporation into this semiconductor include implantation into bulk Si[6] or porous Si,[7] the co-deposition of erbium and silicon thin films,[8] and, more recently in our laboratories, the kinetic trapping of erbium ions during the nucleation and growth of silicon nanoparticles in the gas phase.[9] In terms of nanoparticle structure, it has been determined that the dark features observed in conventional bright field transmission electron microscopy (TEM) are actually aggregates of discrete erbium-containing cubic Si nanocrystals whose average size can be altered by the length of the oven employed in the pyrolysis process.[9b] As an alternative nanocrystal structural motif, we have also recently succeeded in preparing silicon core nanocrystals with erbium-rich shells by the initial pyrolysis of disilane to produce nucleation and growth of the Si core followed by a second thermal annealing step in the presence of a volatile erbium complex.[10]

The oxide surface composition of the Er-doped Si nanocrystals prepared in our laboratories dictates a useful solubility that is present only in ethylene glycol. Thus, we report here studies concerning the surface derivatization of Er-doped Si nanoparticles. The motivation behind such surface modification processes is to increase the general solubility of the doped nanoclusters in a variety of solvents such that facile processing for diverse applications is possible. Ample precedents exist for the surface derivatization of crystalline group IV nanoparticles[11] as well as II−VI nanostructures,[12] with resultant effects observed in terms of both solubility and photophysics. In this work, we employ conventional TEM for an analysis of microstructure, FT IR spectroscopy for characterization of surface ligands, near-IR photoluminescence (PL) for an analysis of the role of

* To whom correspondence should be addressed. E-mail: j.coffer@tcu.edu.

(1) Iyer, S.; Xie, Y.-H. *Science* **1993**, *260*, 40.
(2) Ennen, H.; Schneider, J.; Pomrenke, G.; Axmann, A. *Appl. Phys. Lett.* **1983**, *90*, 943.
(3) Ennen, H.; Pomrenke, G.; Axmann, A.; Eisele, K.; Haydl, W.; Schneider, J. *Appl. Phys. Lett.* **1985**, *46*, 381.
(4) Benton, J. L.; Michel, J.; Kimerling, L. C.; Jacobson, D. C.; Xie. Y.-H.; Eaglesham, D. J.; Fitzgerald, E. A.; Poate, J. M. *J. Appl. Phys.* **1991**, *70*, 2667.
(5) Adler, D. L.; Jacobson, D. C.; Eaglesham, D. J.; Marcus, M. A.; Benton, J. L.; Poate, J. M.; Citrin, P. H. *Appl. Phys. Lett.* **1992**, *61*, 2181.
(6) Polman, A. *J. Appl. Phys.* **1997**, *82*, 1.
(7) (a) Namavar, F.; Lu, F.; Perry, C. H.; Cremins, A.; Kalkhoran, N.; Soref, R. *J. Appl. Phys.* **1995**, *77*, 4813. (b) Hömmerich, U.; Namavar, F.; Cremins, A.; Bray, K. *Appl. Phys. Lett.* **1996**, *68*, 1951. (c) Tsybeskov, L.; Duttagupta, S.; Hirschman, K.; Fauchet, P.; Moore, K.; Hall, D. *Appl. Phys. Lett.* **1997**, *70*, 1790. (d) Lopez, H. A.; Fauchet, P. M. *Appl. Phys. Lett.* **1999**, *75*, 3989. (e) Lopez, H. A.; Fauchet, P. M. *Appl. Phys. Lett.* **2000**, *77*, 3704.
(8) Thilderkvist, A.; Michel, J.; Ngiam, S.; Kimerling, L.; Kolenbrander, K. *Mater. Res. Soc. Symp. Proc.* **1995**, *405*, 265.
(9) (a) St. John, J.; Coffer, J. L.; Chen, Y.; Pinizzotto, R. F. *J. Am. Chem. Soc.* **1999**, *121*, 1888. (b) St. John, J.; Coffer, J. L.; Chen, Y.; Pinizzotto, R. F. *Appl. Phys. Lett.* **2000**, *77*, 1635.
(10) Senter, R.; Chen, Y.; Coffer, J.; Tessler, L. *Nano Lett.* **2001**, *1*, 383.
(11) (a) Yang, C.-S.; Bley, R. A.; Kauzlarich, S. M.; Lee, H. H. W.; Delgado, G. R. *J. Am. Chem. Soc.* **1999**, *121*, 5191. (b) Yang, C.-S.; Liu, Q.; Kauzlarich, S. M.; Phillips, B. *Chem. Mater.* **2000**, *12*, 983. (c) Yang, C.-S.; Kauzlarich, S. M.; Yang, Y. C. *Chem. Mater.* **1999**, *11*, 3666.
(12) (a) Spanhel, L.; Haase, M.; Weller, H.; Henglein, A. *J. Am. Chem. Soc.* **1987**, *109*, 5649. (b) Kortan, A. R.; Hull, R.; Opila, R.; Bawendi, M. G.; Steigerwald, M. L.; Carroll, P. J.; Brus, L. E. *J. Am. Chem. Soc.* **1990**, *112*, 1327. (c) Kuno, M.; Lee, J.; Dabbousi, B.; Mikulec, F.; Bawendi, M. *J. Chem. Phys.* **1997**, *106*, 9869. (d) Dabbousi, B.; Rodriguez-Viejo, J.; Mikulec, F.; Heine, J.; Mattoussi, H.; Ober, R.; Jensen, K.; Bawendi, M. *J. Phys. Chem. B* **1997**, *101*, 9463.

10.1021/cm010644l CCC: $20.00
Published on Web 11/14/2001

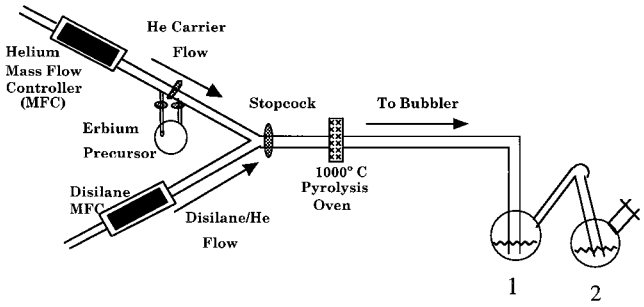

Figure 1. Dual bubbler aerosol reactor design for the synthesis of surface-modified, Er-doped silicon nanocrystals. The surface-capping reagent (dissolved in butylphenyl ether) is placed in bubbler 1; bubbler 2 contains ethylene glycol.

surface-capping moiety on photophysics, and electronic absorption spectroscopy (in the UV−vis region) for an estimate of nanoparticle solubility.

Experimental Section

Nanoparticle Synthesis. While several common routes for the preparation of homogeneous Si nanoparticles are known in the literature,[13−18] the preparation of rare-earth-doped nanoparticles in our lab involves a modification of a high-temperature aerosol reaction involving the combustion of disilane (Si_2H_6, diluted in He carrier gas) and isolation as a colloidal solution in a dual collection bubbler downstream from the pyrolysis oven.[14] The pyrolysis oven has a fixed length of 6 cm and is operated at 1000 °C. Gas flow is regulated by mass-flow controllers (MKS Inc.). The erbium precursor $Er(tmhd)_3$, (tmhd = 2,2,6,6-tetramethyl-3,5-heptanedionato) carried by He gas (Praxair, UHP grade, maintained at a flow rate of 3000 sccm), is mixed with disilane/He (0.48% Si_2H_6, diluted in He carrier gas at flow rate of 3.2 sccm) before reaching the oven (see Figure 1). Necessary reagents for surface derivatization ((3-aminopropyl)triethoxysilane (Gelest), trimethylsilyl acetate, and 4-(triethoxysilyl)-butyronitrile (Aldrich)) are placed in the first bubbler along with the collection solvent (butylphenyl ether or ethylene glycol). The pyrolysis reaction is typically allowed to proceed approximately for 12 h. After initial separation by centrifugation, the supernatant (nanoparticles in butylphenyl ether or ethylene glycol) is treated with a 10-fold excess of THF or hexane to force precipitation of the nanoparticles. The product is washed with additional THF/EtOH (or hexane) to remove physisorbed erbium ions and subsequently dried under vacuum.

Instrumentation. Structural characterization of Er^{3+}-doped Si nanocrystal aggregates was performed using a JEOL 200CX TEM at the University of North Texas. Samples were deposited on carbon films on copper grids, and the ethylene glycol was allowed to evaporate prior to imaging. X-ray energy dispersive spectroscopy (XEDS) analyses of Er^{3+}-doped Si aggregates were performed in the scanning transmission electron microscopy mode. Selected area electron diffraction (SAD) patterns were obtained during TEM analyses.

Silicon concentrations were quantified with the help of the corresponding UV−vis absorption spectra, obtained by using a Hewlett-Packard 8452A diode array spectrometer. In the absence of strong quantum size effects, Mie theory provides a useful estimate of Si concentration by the measurement of optical density at 295 nm, with 1 mg of Si/cm^3 corresponding to a optical density of 1.85 for a 1 mm path length.[14] FT IR spectra were obtained using a MIDAC Corp. IR spectrometer. Low-resolution (±4 nm) near-IR PL spectra were obtained by using an Applied Detector Corp. liquid N_2-cooled Ge detector in conjunction with a Stanford Research Systems Chopper/Lock-In amplifier and an Acton Research Corp. 0.25 m monochromator. Excitation was provided by a Coherent Ar^+ laser. A 10 cm lens was used to focus the light emitted from the samples onto the monochromator entrance slit. Emitted light was collected at 45° relative to the excitation direction. A 1000 nm cutoff filter (Melles Griot) was positioned over the monochromator entrance slit to filter out second- and third-order light. For comparisons of the PL efficiency for nanocrystals with different surface caps, all samples were measured after being dispersed in KBr at a concentration of 10% (by mass) with identical acquisition parameters, i.e., laser power (240 mW), chopping frequency, detector sensitivity, etc.

Scheme 1. Reaction Scheme of Capping Reagents with Si Nanoparticles

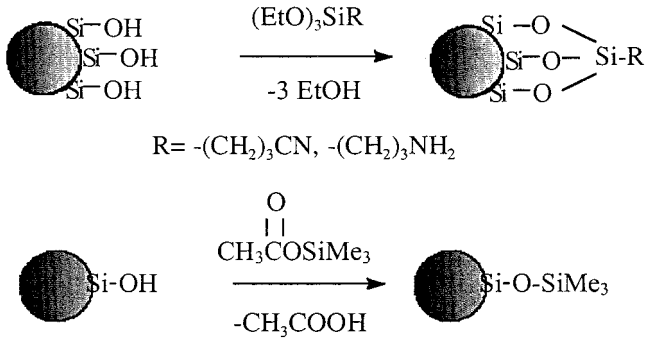

Results and Discussion

The presence of numerous hydroxyl groups on the surface of the as-formed Si nanoparticles and the associated aggregation behavior thereof are presumably major factors in the limited solubility of such species in solvents other than ethylene glycol. Evidence for such effects can be discerned by a strong absorption at 3300 cm^{-1} in the IR vibrational spectra of the Er-doped Si nanocrystals as well as an inspection of corresponding conventional bright field TEM images (vide infra). The focus of our synthetic approach is, therefore, to change the surface composition of the nanocrystals in an attempt to alter the aggregation tendency of the nanoparticles in other common organic solvents. In this initial study, three compounds were used as capping reagents to react with the nanoparticles to convert the hydroxyl group −OH to −OR (R = Silyl). The capping reagents were chosen such that the derivatized nanoparticles would have terminal groups with slightly different polarities, i.e., $-SiMe_3$, $-Si(CH_2)_3CN$, and $-Si(CH_2)_3NH_2$ (Scheme 1).

Initial attempts at surface modification involved reactions of isolated, purified Er-doped Si nanocrystals suspended in dry THF and mixed with a given capping reagent at reflux temperature. At the end of the reaction period (typically on the order of 2−6 h), analysis of the reaction product yielded no evidence for significant capping substitution reactions at the nanoparticle surface, as evidenced by an absence of change in the IR spectrum and solubility properties of the nanocrystals. This would suggest that these reaction conditions are inadequate for the detection of a measurable concentration of new surface ligands or alternatively that the few

(13) Werwa, E.; Seraphin, A. A.; Chiu, L. A.; Zhou, C.; Kolenbrander, K. D. *Appl. Phys. Lett.* **1994**, *64*, 1821.
(14) Littau, K.; Szajowski, P.; Muller, A.; Kortan, A.; Brus. L. *J. Phys. Chem.* **1993**, *97*, 1224.
(15) Brus, L.; Szajowski, P.; Wilson, W.; Harris, T.; Schupler, S.; Citrin, P. *J. Am. Chem. Soc.* **1995**, *117*, 2915.
(16) Wilson, W. L.; Szajowski, P. F.; Brus, L. E. *Science* **1993**, *262*, 1242.
(17) Murthy, T.; Miyamoto, N.; Shibo, M.; Nishizawa, J. *J. Cryst. Growth* **1976**, *33*, 1.
(18) Bley, R. A.; Kauzlarich, S. *J. Am. Chem. Soc.* **1996**, *118*, 12461.

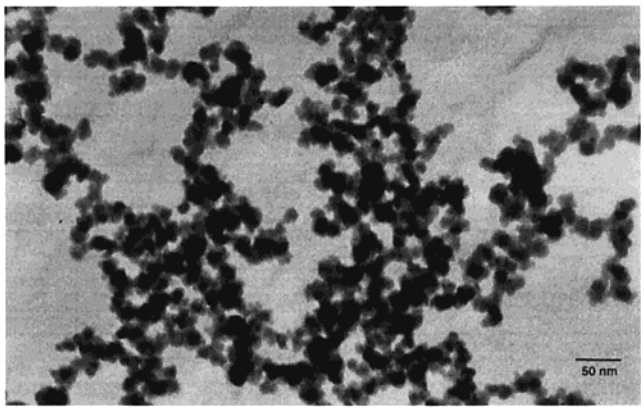

Figure 2. Conventional bright field transmission electron micrograph of an Er-doped Si nanocrystalline sample collected in the presence of trimethylsilyl chloride. The dark contrast areas contain Er.

Table 1. Statistical Data for Er-Doped Si Nanostructure Size as a Function of Capping Group

capping group	avg structure size (nm)	std deviation
noncapped[9]	15.2	6.6
$-SiMe_3$	17.3	2.5
$-Si(CH_2)_3CN$	16.1	2.3
$-Si(CH_2)_3NH_2$	17.9	2.9

new surface bonds that are formed are relatively unstable under workup.

To overcome these difficulties, the surface derivatization reactions were carried out as the nanoparticles were being collected in the bubbler immediately after their formation in the pyrolysis oven. In this design, the capping reagent is mixed with butylphenyl ether as the collecting solvent in the first bubbler (Figure 1).

The determination of the average structure size of the nanoparticles isolated under the above conditions was carried out by using conventional bright field TEM (Figure 2). The average diameter for samples with different capping groups was determined by measuring 200−300 individual structures for each sample (Table 1). As expected, the mean diameter is relatively independent of surface cap and comparable to that of the original, oxide-capped Er-doped Si nanocrystallites synthesized under comparable conditions ($d_{mean} = 17.1$ nm). Interestingly, it appears that the capped nanoparticles do possess a slightly more uniform size distribution (i.e., smaller standard deviations) than that of oxide-capped structures, presumably as a consequence of aggregation inhibition and, hence, ease of imaging (vide infra). SAD measurements carried out concurrently during the TEM measurements confirm that the nanostructures are of the diamond cubic silicon phase and not of an associated silicide or oxide phase.[9]

While XEDS measurements confirm the presence of the erbium dopant, it is important to note that these capped materials also demonstrate the necessary Er^{3+} near-IR PL at 1540 nm at room temperature. This is illlustrated in Figure 3 for the case of Er-doped Si nanocrystals capped with trimethylsilyl moieties. This emission maximum corresponds to the $(^4I_{13/2}) \rightarrow (^4I_{15/2})$ ligand field transition associated with the Er^{3+} centers, with excitation provided via energy transfer from the Si exciton.[9,19,20] Similar measurements for the other surface caps ($-Si(CH_2)_3CN$ and $-Si(CH_2)_3NH_2$) provide

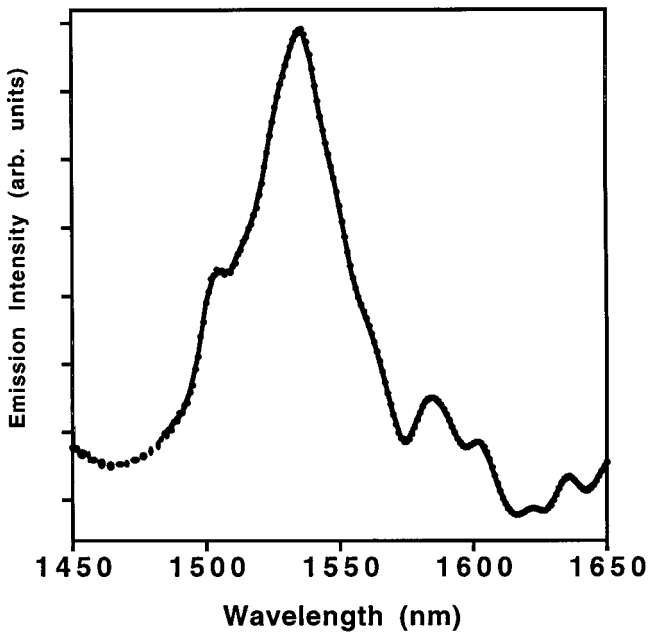

Figure 3. Room-temperature photoluminescence spectrum of trimethylsilyl-capped Er-doped Si nanoparticles dispersed in a KBr matrix. The near-IR emission near 1540 nm is obtained with Ar^+ laser excitation ($\lambda_{ex} = 488$ nm).

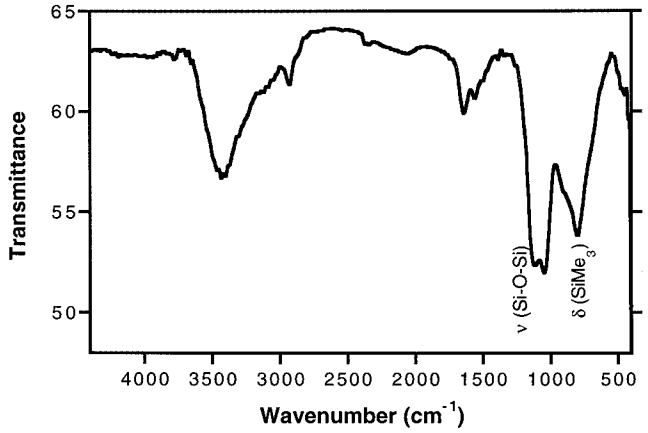

Figure 4. FT IR spectrum of the trimethylsilyl-capped, Er-doped Si nanocrystals dispersed in KBr.

comparable intensities for the PL emanating from the Er^{3+} centers. However, it should be noted that the nature of these derivatization species apparently introduces some additional nonradiative pathways for electron−hole recombination as the relative quantum efficiency for the erbium fluorescence of these surface-modified nanocrystals is approximately one-fifth that of the original, oxide-capped material.

Evidence for modification of the nanocrystal surface composition comes in part from IR vibrational spectroscopy. While the extent of passivation is not complete (e.g., some oxide in the form of Si−O−Si at 1100 cm^{-1}), for the case of the trimethylsilyl cap, a distinct shift in the δ (Si−CH_3) deformation mode (~50 cm^{-1} relative to the free surface cap) is seen at ca. 805 cm^{-1} (Figure 4). Visually striking proof of surface modification also comes from an assessment of solubility changes as a

(19) Franzo, G.; Pacifici, D.; Vinviguerra, V.; Priolo, F.; Iacona, F. *Appl. Phys. Lett.* **2000**, *76*, 2167.
(20) Kik, P. G.; Polman, A. *J. Appl. Phys.* **2000**, *88*, 1992.

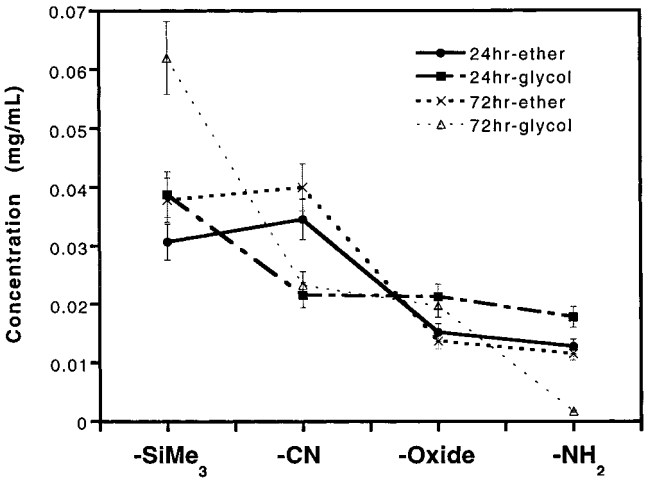

Figure 5. Differential solubility of derivatized Er-doped Si nanoparticles as a function of surface-capping moiety and solvent (ethylene glycol and butylphenyl ether). Changes in solubility as a function of time (24 vs 72 h) for these solvents are also shown.

function of capping moiety. For example, a solution of the reaction product containing doped Si nanocrystals with the trimethylsilyl cap collected in phenylbutyl ether retains a deep brown color after 72 h, in marked contrast to the butylamine-capped product which clearly flocculates into an insoluble brown solid during the same time period in this solvent. This is likely to be a consequence of hydrogen-bonding-induced aggregation by the primary amine functional group between nanoparticles.

These differential solubility measurements can be quantified with the help of electronic absorption spectroscopy. Figure 5 shows the dependence of the solubility of the derivatized Er-doped Si nanoparticles on the capping moiety. In this case, Si concentrations were measured on the basis of the known optical density of Si (from Mie theory) at 295 nm.[14] This figure clearly shows that the nanoparticles treated with less hydrophilic capping reagents have better solubility in both ethylene glycol and butylphenyl ether, with structures capped with $-SiMe_3$ groups demonstrating the highest concentrations in the solvents tested. These measurements also confirm the visual differences in solubility between nanoparticles with $-NH_2$ as the end groups and that of the $-SiMe_3$/$-Si(CH_2)_3CN$-capped nanoparticles noted earlier, indicating that nonpolar terminal groups on a given nanoparticle surface can reduce the extent of their aggregation in these solvents.

Another important issue to glean from these data is the change in Si concentration as the solutions age upon exposure to excess solid Er-doped Si nanocrystals. In ethylene glycol, the solubility of the trimethylsilyl-capped nanocrystals actually increases upon standing (from 24 to 72 h), while that of the alkylamine moeities drops essentially to zero in the same time interval. An increase in solubility is also observed for $-Si(CH_2)_3CN$-capped nanoparticles dissolved in butylphenyl ether as a function of time, albeit at a lesser magnitude. Again, such phenomena are consistent with the interfacial properties of a given capping moiety in these specific solvents.

In summary, it is found that some variation in Er-doped silicon nanocrystallite solubility in selected solvents can be achieved by surface derivatization reactions in the product collection bubbler upon the pyrolysis of disilane and an Er^{3+} source in a dilute helium stream. Greater solubility in solvents that are relatively more volatile than ethylene glycol should facilitate their use as precursors in the formation of extended photonic structures via infiltration methods.[21] The ability to work with these nanocrystals in a wider variety of solvents may also lead to routes for their solubility in aqueous solutions, and applications relevant to biological labeling[22] or delivery may now be possible. Experiments along these lines are underway.

Acknowledgment. We gratefully acknowledge the National Science Foundation (DMR-9819178) and the Robert A. Welch Foundation for financial support of this research.

CM010644L

(21) (a) For a brief review for metals, see: Kulinowski, K.; Jiang, P.; Vaswani, H.; Colvin, V. *Adv. Mater.* **2000**, *12*, 833. (b) For semiconductors, see: Vlasov, Yu. A.; Yao, N.; Norris, D. J. *Adv. Mater.* **1999**, *11*, 165.

(22) (a) Chan, W. C. W.; Nie, S. *Science* **1998**, *281*, 2016. (b) Bruchez, M. J.; Moronne, M.; Gin, P.; Weiss, S.; Alivisatos, P. A. *Science* **1998**, *281*, 2013. (c) Lacoste, T. D.; Michalet, X.; Pinaud, F.; Chemla, D. S.; Alivisatos, A. P.; Weiss, S. *Proc. Natl. Acad. Sci. U.S.A.* **2000**, *97*, 9461.